

# Adaptive Control for Ionic Polymer-Metal Composite Actuator Based on Continuous-Time Approach <sup>\*</sup>

Xinkai Chen <sup>\*</sup>

<sup>\*</sup> *Shibaura Institute of Technology, Saitama-shi, Saitama 337-8570, Japan  
(E-mail: chen@shibaura-it.ac.jp).*

**Abstract:** This paper discusses the model reference adaptive control problem for ionic polymer-metal composite (IPMC) actuators. Firstly, a mathematical model of the IPMC actuator is constructed as a stable second order dynamical system preceded by a hysteresis representation. Then, an adaptive controller is synthesized for the IPMC actuator. The proposed control law ensures the global stability of the controlled IPMC system, and the position error of IPMC actuator can be controlled by choosing the design parameters. Experimental results confirm the effectiveness of the proposed method.

## 1. INTRODUCTION

Ionic polymer-metal composites (IPMCs) form an important category of electroactive polymers and have actuation capability known as artificial muscles (Nemat-Nasser and Li, 2000; Shahinpoor and Kim, 2001; Bar-Cohen, 2004). An IPMC sample typically consists of a thinion-exchange membrane, chemically plated on both surfaces with a noble metal as electrode. Transport of hydrated cations and water molecules within an IPMC under an applied voltage and the associated electrostatic interactions lead to bending motions of the IPMC, and hence the actuation effect. Fig. 1 illustrates the mechanism of the IPMC actuation. Because of the softness, resilience, biocompatibility, and the capability of producing large deformation and large force under a low action voltage, IPMCs are very attractive for many applications in the fields of biomedical devices and biomimetic robots (Chen and Tan, 2008; Chen and Tan, 2010). Microfabrication of IPMC has also been extends to micro- and nanomanipulation domains. However, the main disadvantage is the hysteresis phenomenon between the applied electric voltage and the displacement (Fig. 2). Due to the undifferentiable and nonmemoryless character of the hysteresis, it causes position errors which limit the operating speed and precision of IPMCs. The development of control techniques to mitigate the effects of hysteresis has been studied for decades and has recently re-attracted significant attention. Interest in studying dynamic systems with actuator hysteresis is motivated by the fact that they are nonlinear system with nonsmooth nonlinearities for which traditional control methods are insufficient and thus require development of alternate effective approaches.

About the challenge of the problem, the thorough characterization of the hysteresis forms the foremost task (Banks, 2000; Guyer, et al, 1994; Oh and Bernstein, 2007; Webb, et al, 1998). Appropriate hysteresis models may then be applied to describe the nonsmooth nonlinearities for their potential usage in formulating the control algorithms. The basic idea consists of the modeling of the real complex hysteresis nonlinearities by the

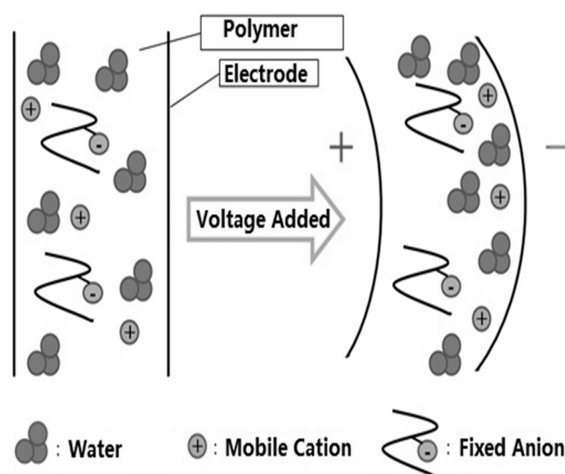


Fig. 1. Mechanism of IPMC actuation

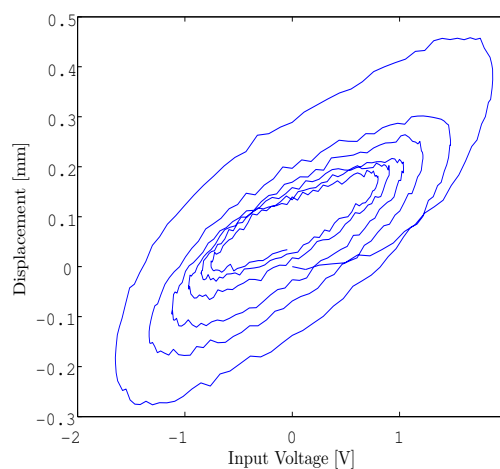


Fig. 2. The relation between the applied electric voltage and the displacement of IPMC actuator

weighted aggregate effect of all possible so-called elementary hysteresis operators. Elementary hysteresis operators are non-

<sup>\*</sup> This work is partially supported by JSPS Grants-in-Aid for Scientific Research C-24560553, Funds for Natural Science Foundation of China under Grant 61074097 and 61228301, and State Key Laboratory of Synthetical Automation for Process Industries (Northeastern University), China.

complex hysteretic nonlinearities with a simple mathematical structure. The popular models are Preisach model (Croft, et al, 2001; Cross, et al, 2001; Mayergoyz, 1991; Natale, et al, 1991), Prandtl-Ishlinskii (PI) model (Brokate and Sprekels, 1996; Visintin, 1994), and Krasnosel'skii-Pokrovskii (KP) model (Krasnosel'skii and Pokrovskii, 1989; Visintin, 1994). The Preisach model and KP model are parameterized by a pair of threshold variables (Mayergoyz, 1991), whereas the PI model is a superposition of elementary stop (or play) operators which are parameterized by a single threshold variable.

Upon the developments in various hysteresis models, it is by nature to seek means to fuse these hysteresis models with the available control techniques to mitigate the effects of hysteresis, especially when the hysteresis is unknown, which is a typical case in many practical applications. However, the results on the fusion of the available hysteresis models with the available control techniques is surprisingly sparse in the literature (Su, et al, 2005; Tan and Baras (2004); Tao and Kokotovic, 1995)). The most common approach in coping with hysteresis in the literature is to construct an inverse operator, which is pioneered by Tao and Kokotovic (1995), and the reader may refer to, for instance Moheimani and Goodwin (2001), Iyer and Shirley (2004), Krejci and Kuhnen (2001), Kuhnen and Janocha (1999), and the references therein. Essentially, the inversion problem depends on the phenomenological modeling methods (for example, using Preisach models). Due to multi-valued and non-smooth features of hysteresis, the inversion always generates errors and possesses strong sensitivity to the model parameters. These errors directly make the stability analysis of the closed-loop system very difficult except for certain special cases. Another approach, instead of directly constructing the inversion from the hysteresis model, is an approximate implicit inversion. This method, associated with the preceded system, was introduced for convenience of the stability analysis for the closed-loop system (Chen, et al, 2008). The approximate implicit inversion is obtained by searching for an optimal value of the inversion based on a performance index. However, unlike the direct inverse construction approach, this approximate implicit inversion technique is dependent on the preceded system (Chen, et al, 2008). The result is also somewhat preliminary as it is illustrated only for uncertain linear discrete-time systems.

In this paper, a new model for the IPMC actuator is proposed based on phenomenological method. The model is a stable second order dynamical system preceded by a PI hysteresis representation. An adaptive controller is synthesized for the IPMC actuator. The advantage is that only the parameters in the formulation of the controller need to be adaptively estimated, and the real values of the parameters in the IPMC model need to be neither identified nor measured. The proposed control law ensures the global stability of the controlled IPMC actuator, and the position error of IPMC actuator can be controlled by choosing the design parameters. Experimental results confirm the effectiveness of the proposed method.

## 2. PROBLEM STATEMENT

In this paper, the robust control for IPMC actuator shown in Fig. 3 is studied. By observing the measured input-output relation in Fig. 2 (where the input is  $v(t) = \frac{2\sin(2\pi t)}{1+\frac{1}{2}t}$ ), it can be seen that there exists a typical hysteretic behavior between the input voltage and output displacement. In the following, a relatively

simple model will be presented to describe the IPMC actuator in order to be useful in the control design.

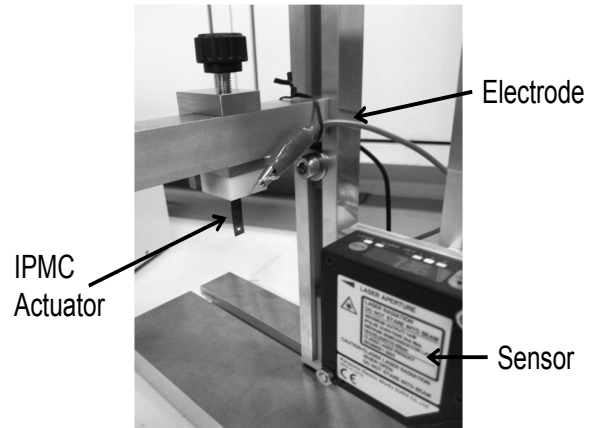


Fig. 3. Experimental setup of IPMC actuator

### 2.1 Prandtl-Ishlinskii Model

In this subsection, a relatively simple hysteresis model "Prandtl-Ishlinskii (PI) operator" will be adopted because of its ability of describing the complicated hysteresis. The basic element of the PI operator is the so-called play operator. For  $w \in \bar{R}$  and arbitrary piece-wise monotone function  $v(t)$ , define  $f_r : \bar{R} \times \bar{R} \rightarrow \bar{R}$  as

$$f_r(v, w) = \max(v - r, \min(v + r, w)) \quad (1)$$

where  $\bar{R}$  denotes the set of real number. For any initial value  $u_{-1} \in \bar{R}$  and  $r \geq 0$ , the play operator  $F_r[v; u_{-1}](t)$  is defined as

$$F_r[v; w_{-1}](0) = f_r(v(0), w_{-1}), \quad (2)$$

$$F_r[v; w_{-1}](t) = f_r(v(t), F_r[v](t_i)) \quad (3)$$

for  $t_i \leq t \leq t_{i+1}$ , where the function  $v(t)$  is monotone for  $t_i \leq t \leq t_{i+1}$ . The play operator is mainly characterized by the threshold parameter  $r \geq 0$  which determines the height of the hysteresis region in the  $(v, u)$  plane.

For simplicity, denote  $F_r[v; w_{-1}](t)$  by  $F_r[v](t)$  in the following development of this note. It should be noted that the play operator  $F_r[v](t)$  is rate-independent.

Based on the above definitions, the PI hysteresis model is then defined as

$$u(t) = \int_0^\infty p(r) F_r[v](t) dr \quad (4)$$

where  $p(r)$  is the density function which is usually unknown, satisfying  $p(r) \geq 0$  with  $\int_0^\infty rp(r)dr < \infty$ . Since the density function  $p(r)$  vanishes for large values of  $r$ , it is reasonable to assume that there exists a constant  $R$  such that  $p(r) = 0$  for  $r > R$ . Thus, model (4) gives

$$u(t) = \int_0^R p(r) F_r[v](t) dr. \quad (5)$$

It should be noted that PI model (5) indeed generates the hysteresis curves and are well-suited to describe complicated hysteretic behaviors.

Fig. 4 shows the hysteresis curves generated by PI model for  $p(r) = e^{-0.1(r-1)^2}$ ,  $v(t) = \frac{2\sin(2\pi t)}{1+\frac{1}{2}t}$ ,  $r \in [0, 20]$ ,  $t \in [0, 3]$ .

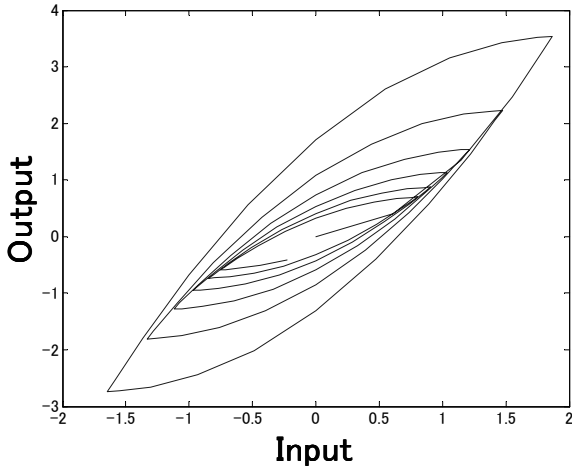


Fig. 4. Hysteresis curves of PI model

### 2.2 Model of IPMC Actuator and Control Purpose

By observing Fig. 4, it can be seen that the PI model is still not capable to describe the hysteresis behavior existing in the IPMC actuator (see Fig. 2), especially at the instants when the input changes its monotonous properties (i.e. from increasing to decreasing, or from decreasing to increasing). For this purpose, a filter  $G(s) = \frac{1}{s^2 + a_1s + a_2}$  will be added to the output of the PI hysteresis to smoothen the sharpness of the PI model (Fig. 5), where  $a_1$  and  $a_2$  are constants and  $s^2 + a_1s + a_2$  is a Hurwitz polynomial. In this figure,  $y(t) \in \bar{R}$  represents the displacement of the IPMC actuator,  $u(t)$  is called the output of the PI hysteresis,  $v(t)$  is the voltage applied to the IPMC actuator.

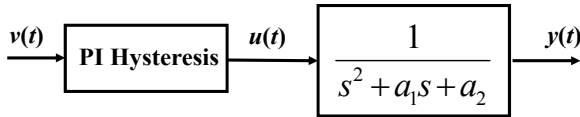


Fig. 5. Model of IPMC actuator

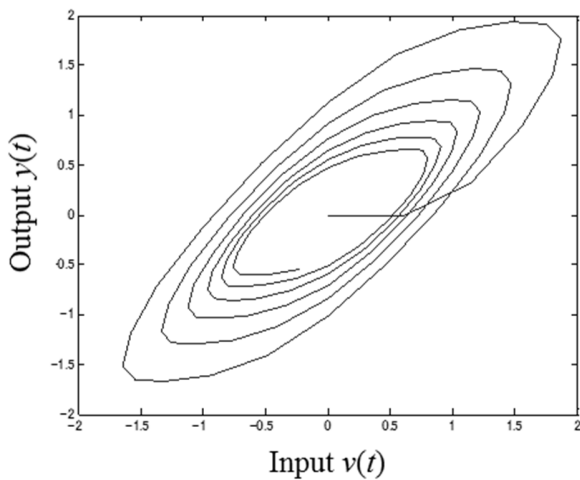


Fig. 6. The relation between  $v(t)$  and  $y(t)$

Fig. 6 shows the relation between  $v(t)$  and  $y(t)$  with  $v(t) = \frac{2\sin(2\pi t)}{1+\frac{2}{t}}$ ,  $p(r) = e^{-0.1(r-1)^2}$ ,  $r \in [0, 20]$ ,  $t \in [0, 3]$ ,  $a_1 = 1$  and  $a_2 = 2$ . It can be seen that the characteristic behavior of Fig. 6 is very similar to that of Fig. 2. Thus, the scheme in Fig 5 can be considered to be well-suited to describe the hysteretic behavior in IPMC actuator. Therefore, IPMC actuator can be modelled as follows.

$$(s^2 + a_1s + a_2)[y](t) = u(t) \quad (6)$$

$$u(t) = \int_0^R p(r)F_r[v](t)dr \quad (7)$$

It should be noted that the parameters  $a_1$  and  $a_2$ , and the density function  $p(r)$  are all unknown in practice.

The objective is to design an adaptive controller so that the input voltage  $v(t)$  can drive the displacement  $y(t)$  of IPMC actuator to track a desired position  $y_m(t)$  of a reference model described by

$$P_m(s)[y_m](t) = r_m(t) \quad (8)$$

where  $r_m(t)$  is the uniformly bounded input of the reference model,  $P_m(s)$  is a monic stable polynomial with degree 2 described as

$$P_m(s) = s^2 + a_{m1}s + a_{m2} \quad (9)$$

where  $a_{m1}$  and  $a_{m2}$  are parameters.

## 3. ADAPTIVE CONTROL DESIGN

### 3.1 Some Preliminaries

To begin with, introduce a positive real number  $\Lambda$ . Now, consider the polynomial equation

$$\begin{aligned} \theta_1(s^2 + a_1s + a_2) + (\theta_2 + \theta_{20}(s + \Lambda)) \\ = (s + \Lambda)(s^2 + a_1s + a_2) - P_m(s) \end{aligned} \quad (10)$$

with  $\theta_1 \in \bar{R}$ ,  $\theta_2 \in \bar{R}$ , and  $\theta_{20} \in \bar{R}$ . It is well known that the parameters  $\theta_1$ ,  $\theta_2$ , and  $\theta_{20}$  exist uniquely. Operating both sides of (10) on  $y(t)$  yields

$$\begin{aligned} \theta_1 u(t) + (\theta_2 + \theta_{20}(s + \Lambda))[y](t) \\ = (s + \Lambda)[u](t) - (s + \Lambda)P_m(s)[y](t) \end{aligned} \quad (11)$$

By observing that the polynomial  $s + \Lambda$  is stable, the relation between the input and the output of the linear plant can also be expressed as

$$u(t) = \theta_1 \frac{1}{s + \Lambda}[u](t) + \theta_2 \frac{1}{s + \Lambda}[y](t) + \theta_{20}y(t) + P_m(s)[y](t) \quad (12)$$

where an exponential decaying term is omitted. Thus, by substituting PI model (5) into (12), it gives

$$\begin{aligned} \int_0^R p(r)F_r[v](t)dr = \int_0^R p(r)\theta_1 \frac{1}{s + \Lambda}[F_r[v]](t)dr \\ + \theta_2 \frac{1}{s + \Lambda}[y](t) + \theta_{20}y(t) + P_m(s)[y](t) \end{aligned} \quad (13)$$

Therefore, it can be easily seen that the exponential output tracking of the linear plant can be achieved if the design input  $v(t)$  to the hysteresis is chosen such that the next equation holds

$$\begin{aligned} \int_0^R p(r)F_r[v](t)dr = \int_0^R p(r)\theta_1 \frac{1}{s + \Lambda}[F_r[v]](t)dr \\ + \theta_2 \frac{1}{s + \Lambda}[y](t) + \theta_{20}y(t) + r_m(t) \end{aligned} \quad (14)$$

### 3.2 Adaptive Control Algorithm

Since the transfer function is unknown, the parameters  $\theta_1$ ,  $\theta_2$ , and  $\theta_{20}$  are all unavailable. Thus, the control input  $v(t)$  which should satisfy (14) can not be determined. It should be noted that the density function  $p(r)$  is also unknown.

In order to derive the control input  $v(t)$ , the unknown parameters needed in the design will be estimated by adaptive algorithms.

Suppose that the estimates of  $p(r)$ ,  $p(r)\theta_1$ ,  $\theta_2$  and  $\theta_{20}$  are respectively  $\hat{p}(r,t)$ ,  $\hat{\theta}_1(r,t)$ ,  $\hat{\theta}_2(t)$  and  $\hat{\theta}_{20}(t)$  at instant  $t$ , where the estimate  $\hat{p}(r,t)$  should be designed such that  $\hat{p}(r,t) \geq 0$  for all  $r$  and  $t$ .

With these estimates, by observing (14), the design task is to find a signal  $v(t)$  as an input of the hysteresis so that the following equation holds

$$\int_0^R \hat{p}(r,t) F_r[v](t) dr = \int_0^R \hat{\theta}_1(r,t) \frac{1}{s+\Lambda} [F_r[v]](t) dr + \hat{\theta}_2(t) \frac{1}{s+\Lambda} [y](t) + \hat{\theta}_{20}(t) y(t) + r_m(t) \quad (15)$$

For simplicity, define

$$W(t) = \int_0^R \hat{\theta}_1(r,t) \frac{1}{s+\Lambda} [F_r[v]](t) dr + \hat{\theta}_2(t) \frac{1}{s+\Lambda} [y](t) + \hat{\theta}_{20}(t) y(t) + r_m(t) \quad (16)$$

Now, we try to find a virtual signal  $\bar{v}(t)$  which should satisfy

$$\int_0^R \hat{p}(r,t) F_r[\bar{v}](t) dr = W(t) \quad (17)$$

Let  $[v_{min}, v_{max}]$  be the practical input range of the IPMC actuator, which is a subset of  $[-R, R]$ . Suppose  $W(t)$  is monotonic on the interval  $t_i \leq t \leq t_{i+1}$ . For each  $t \in [t_i, t_{i+1}]$ , define

$$\int_0^R \hat{p}(r,t) F_r[v_{max}](t) dr = \bar{W}_{sat}(t), \quad (18)$$

$$\int_0^R \hat{p}(r,t) F_r[v_{min}](t) dr = \underline{W}_{sat}(t) \quad (19)$$

Since  $\hat{p}(r,t) \geq 0$ , it holds

$$\underline{W}_{sat}(t) \leq \int_0^R \hat{p}(r,t) F_r[v](t) dr \leq \bar{W}_{sat}(t) \quad (20)$$

for  $v_{min} \leq v(t) \leq v_{max}$ .

Without loss of generality, suppose  $W(t)$  is monotonically increasing on the interval  $t_i \leq t \leq t_{i+1}$ . For each  $t \in [t_i, t_{i+1}]$ , define a new variable  $\bar{v}_\mu(t)$  with  $\bar{v}_0(t) = v(t_i)$  and another new variable  $W_\mu(t)$

$$\bar{v}_\mu(t) = \bar{v}_0(t) + \mu, \quad (21)$$

$$W_\mu(t) = \int_0^R \hat{p}(r,t) F_r[\bar{v}_\mu](t) dr, \quad (22)$$

where  $\mu$  is a parameter varying in the range  $\mu \in [0, v_{max} - v_{min}]$ .

If  $W(t) > \bar{W}_{sat}(t)$ , let  $\bar{v}(t) = v_{max}$ .

If  $W(t) < \underline{W}_{sat}(t)$ , let  $\bar{v}(t) = v_{min}$ .

If  $\underline{W}_{sat}(t) \leq W(t) \leq \bar{W}_{sat}(t)$ , the value of  $\bar{v}(t)$  is derived from the following algorithm.

**Step 1:** Let  $\mu$  increase from 0.

**Step 2:** Calculate  $\bar{v}_\mu(t)$  and  $W_\mu(t)$ . If  $W_\mu(t) < W(t)$ , then let  $\mu$  increase continuously and go to Step 2; Otherwise, go to Step 3.

**Step 3:** Stop the increasing of  $\mu$ , memorize it as  $\mu_0$  and define  $\bar{v}(t) = \bar{v}_{\mu_0}(t)$ .

For  $t = 0$ ,  $\bar{v}_0(0)$  can be defined as  $\bar{v}_0(0) = v_{min}$ . The calculated  $\bar{v}(t)$  is called the ‘‘implicit inversion’’ of  $W(t)$ .

With the above implicit inversion, the adaptive control  $v(t)$  as an input of the hysteresis can thus be chosen as

$$v(t) = \bar{v}(t) \quad (23)$$

Therefore, the determined adaptive control  $v(t)$  satisfies (15) if  $\underline{W}_{sat}(t) \leq W(t) \leq \bar{W}_{sat}(t)$ .

To apply the adaptive control law (23), it is necessary to develop algorithms to estimate the required parameters  $\hat{p}(r,t)$ ,  $\hat{\theta}_1(r,t)$ ,  $\hat{\theta}_2(t)$  and  $\hat{\theta}_{20}(t)$  in (15). Define

$$e(t) = y(t) - y_m(t) \quad (24)$$

If  $\underline{W}_{sat}(t) \leq W(t) \leq \bar{W}_{sat}(t)$ , from (8), (13) and (15), it yields

$$e(t) = \frac{1}{P_m(s)} \left[ - \int_0^R \tilde{p}(r, \cdot) F_r[v] dr + \int_0^R \tilde{\theta}_1(r, \cdot) \frac{1}{s+\Lambda} [F_r[v]] dr + \tilde{\theta}_2 \frac{1}{s+\Lambda} [y] + \tilde{\theta}_{20} y \right] (t) \quad (25)$$

with  $\tilde{p}(r,t) = \hat{p}(r,t) - p(r)$ ,  $\tilde{\theta}_1(r,t) = \hat{\theta}_1(r,t) - p(r)\theta_1$ ,  $\tilde{\theta}_2(t) = \hat{\theta}_2(t) - \theta_2$  and  $\tilde{\theta}_{20}(t) = \hat{\theta}_{20}(t) - \theta_{20}$ , where an exponential decaying term is omitted.

Now, introduce a first order monic stable polynomial  $s+L$  such that  $\frac{s+L}{P_m(s)}$  is strictly positive real, and define a new error  $\varepsilon(t)$  as

$$\varepsilon(t) = e(t) + \frac{s+L}{P_m(s)} [\xi - \kappa \varepsilon m_0^2] (t) \quad (26)$$

where  $\kappa > 0$  is an arbitrary constant, and

$$\begin{aligned} \xi(t) = & - \int_0^R \hat{p}(r,t) \frac{1}{s+L} [F_r[v]](t) dr - \frac{1}{s+L} [\zeta](t) \\ & + \int_0^R \hat{\theta}_1(r,t) \frac{1}{(s+L)(s+\Lambda)} [F_r[v]](t) dr \\ & + \hat{\theta}_2(t) \frac{1}{(s+L)(s+\Lambda)} [y](t) + \hat{\theta}_{20}(t) \frac{1}{s+L} [y](t), \end{aligned} \quad (27)$$

$$\begin{aligned} \zeta(t) = & - \int_0^R \hat{p}(r,t) F_r[v](t) dr \\ & + \int_0^R \hat{\theta}_1(r,t) \frac{1}{s+\Lambda} [F_r[v]](t) dr \\ & + \hat{\theta}_2(t) \frac{1}{s+\Lambda} [y](t) + \hat{\theta}_{20}(t) y(t), \end{aligned} \quad (28)$$

$$\begin{aligned} m_0(t) = & \left( \int_0^R \left\| \frac{1}{(s+L)(s+\Lambda)} [F_r[v]](t) \right\|^2 dr \right. \\ & + \int_0^R \left( \frac{1}{s+L} [F_r[v]](t) \right)^2 dr + \xi^2(t) \\ & \left. + \left\| \frac{1}{(s+L)(s+\Lambda)} [y](t) \right\|^2 + \left( \frac{1}{s+L} [y](t) \right)^2 \right)^{\frac{1}{2}} \end{aligned} \quad (29)$$

The parameter adaptation laws with projection are chosen as

$$\dot{\hat{p}}(r,t) = \begin{cases} \gamma_0 \varepsilon(t) \frac{1}{s+L} [F_r[v]](t) & \text{if } \hat{p}(r,t) > 0 \\ \gamma_0 \varepsilon(t) \frac{1}{s+L} [F_r[v]](t) & \text{if } \hat{p}(r,t) = 0 \text{ and} \\ 0 & \varepsilon(t) \frac{1}{s+L} [F_r[v]](t) > 0 \\ & \text{otherwise} \end{cases} \quad (30)$$

$$\dot{\hat{\theta}}_1(r,t) = -\Gamma \varepsilon(t) \frac{1}{(s+L)(s+\Lambda)} [F_r[v]](t), \quad (31)$$

$$\dot{\hat{\theta}}_2(t) = -B \varepsilon(t) \frac{1}{(s+L)(s+\Lambda)} [y](t), \quad (32)$$

$$\dot{\hat{\theta}}_{20}(t) = -\beta \varepsilon(t) \frac{1}{s+L} [y](t) \quad (33)$$

where  $\gamma_0 > 0$ ,  $\Gamma = \Gamma^T > 0$ ,  $B = B^T > 0$ ,  $\beta > 0$  are the adaptation gains.

**Lemma 1:** If  $W_{sat}(t) \leq W(t) \leq \bar{W}_{sat}(t)$ , the adaptive laws (30)-(33) guarantee that  $\varepsilon(t) \in L^2 \cap L^\infty$ ,  $\varepsilon(t)m_0(t) \in L^2$ ,  $\hat{p}(r,t) \in L^\infty$ ,  $\hat{\theta}_1(r,t) \in L^\infty$ ,  $\hat{\theta}_2(t) \in L^\infty$ ,  $\hat{\theta}_{20}(t) \in L^\infty$ ,  $\dot{\hat{p}}(r,t) \in L^2$ ,  $\dot{\hat{\theta}}_1(r,t) \in L^2$ ,  $\dot{\hat{\theta}}_2(t) \in L^2$ , and  $\dot{\hat{\theta}}_{20}(t) \in L^2$ .

**Proof:** If  $W_{sat}(t) \leq W(t) \leq \bar{W}_{sat}(t)$ , then, from (25) and (26), it gives

$$\varepsilon(t) = \frac{s+L}{P_m(s)} [\sigma](t) \quad (34)$$

with

$$\begin{aligned} \sigma(t) = & \int_0^R \tilde{\theta}_1^T(r,t) \frac{1}{(s+L)(s+\Lambda)} [F_r[v]](t) dr \\ & + \tilde{\theta}_2^T(t) \frac{1}{(s+L)(s+\Lambda)} [y](t) + \tilde{\theta}_{20}(t) \frac{1}{s+L} [y](t) \\ & - \int_0^R \tilde{p}(r,t) \frac{1}{s+L} (s) [F_r[v]](t) dr - \kappa \varepsilon(t) m_0^2(t). \end{aligned} \quad (35)$$

Let the controllable realization of  $\frac{L(s)}{P_m(s)}$  be  $(A, b, c)$  and  $x_\varepsilon(t)$  be its state variable. Then, from (34), it yields

$$\dot{x}_\varepsilon(t) = Ax_\varepsilon(t) + b\sigma(t), \quad \varepsilon(t) = cx_\varepsilon(t). \quad (36)$$

Since  $\frac{s+L}{P_m(s)}$  is strictly positive real, it follows from the Lefschetz-Kalman-Yakubovich Lemma that there exist real constant matrices  $P = P^T > 0$ ,  $Q = Q^T > 0$  such that

$$A^T P + PA = -Q, \quad Pb = c^T. \quad (37)$$

Consider the positive definite function

$$\begin{aligned} V(t) = & x_\varepsilon^T P x_\varepsilon + \int_0^R \frac{1}{\gamma_0} \tilde{p}^2(r,t) dr + \int_0^R \tilde{\theta}_1^T(r,t) \Gamma^{-1} \tilde{\theta}_1(r,t) dr \\ & + \tilde{\theta}_2^T(t) B^{-1} \tilde{\theta}_2(t) + \frac{1}{\beta} \tilde{\theta}_{20}^2(t). \end{aligned} \quad (38)$$

By differentiating  $V(t)$ , the lemma can be proved.

**Theorem 1:** If  $W_{sat}(t) \leq W(t) \leq \bar{W}_{sat}(t)$ , all the signals in the closed-loop system consisting of the linear plant (6), the hysteresis (7), the reference model (8), the controller (23) and the adaptive laws (30)-(33) are bounded and the output tracking error  $e(t) = y(t) - y_m(t)$  satisfies  $e(t) \in L^2$  and  $\lim_{t \rightarrow \infty} e(t) \rightarrow 0$ .

**Proof:** Due the page limitation, the proof is omitted.

#### 4. EXPERIMENTAL RESULTS

The experimental setup of IMPC actuator is shown in Fig. 3.

The control purpose is to drive the output  $y(t)$  of the nano-positioner to track the output  $y_m(t)$  of the reference model described by  $(s+1)(s+2)[y_m](t) = r_m(t)$ .

In the adaptive control experiment,  $\Lambda(s)$  is chosen as  $\Lambda(s) = s+3$ ,  $L(s)$  is chosen as  $L(s) = s+1.5$ , the initial values are chosen as  $\hat{p}(r,0) = 0.1$ ,  $\hat{\theta}_1(r,0) = 0.2$ ,  $\hat{\theta}_2(0) = 0.2$ ,  $\hat{\theta}_{20}(0) = 0.2$ .

The sampling period is chosen as 0.025 s. The experiment is conducted for the reference input  $r_m(t) = \sin(0.4t)$ . The desired output  $y_m(t)$  is shown in Fig. 7.

The design parameters are shown in Table.1. The estimated parameter  $\hat{\theta}_1(r,t)$  for  $r = 0.2$  is shown in Fig. 8. For other values of  $r$ , the convergence has also been confirmed. Similarly, the convergences of other parameters have also been observed. The control input is shown in Fig. 9. The output tracking error is shown in Fig. 10. It can be seen that the output convergence is confirmed in a relatively short time and the steady state error is within 0.01mm.

It should be noted that good output trackings for the cases that  $r_m(t)$  is constant or piecewise constant have also been verified by experimental results.

Table 1. Control Parameter Values

Parameters	Values
$R$	20
$L$	1.5
$\Gamma$	800
$\gamma_0$	800
$B$	800
$\beta$	10
$\kappa$	0.01

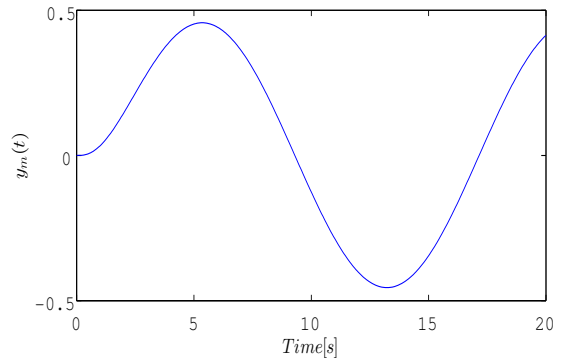


Fig. 7. Desired output  $y_m(t)$

#### 5. CONCLUSION

This paper has discussed the adaptive control for IPMC actuator. A simple continuous-time model which is a stable second order dynamical system preceded by a PI hysteresis representation has been formulated for the IPMC actuator. The model reference adaptive control has been synthesized based on the obtained mathematical model, and it can also ensure the stability of the controlled IPMC system. The high precision output

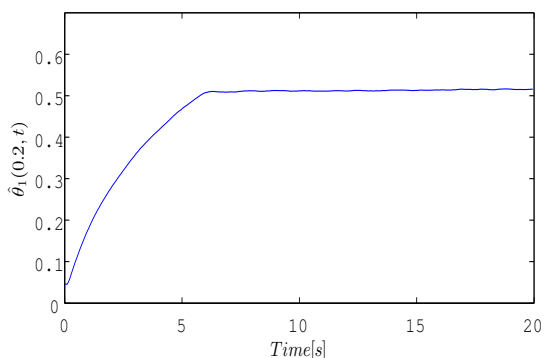


Fig. 8. Estimated parameter  $\hat{\theta}_1(r, t)$  for  $r = 0.2$

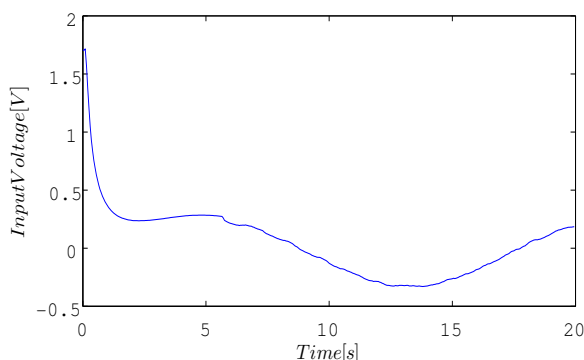


Fig. 9. The control input  $v(t)$

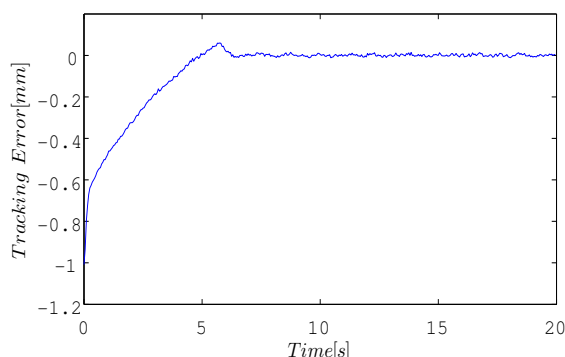


Fig. 10. Output tracking error  $y(t) - y_m(t)$

tracking control has been confirmed by experimental results for low frequency desired signals. The high frequency output tracking control is expected to be conducted in the future.

#### REFERENCES

Banks, H.T. and Smith, R.C. Hysteresis modeling in smart material systems. *J. Appl. Mech. Eng.*, vol. 5, pp. 31-45, 2000.

Bar-Cohen, Y. Electric flex. *IEEE Spectrum*, vol. 41, no. 6, pp. 29-33, 2004.

Brokate, M. and Sprekels, J. Hysteresis and Phase Transitions. New York: Springer-Verlag, 1996.

Chen, X., Su, C.-Y., and Fukuda, T. Adaptive control for the systems preceded by hysteresis. *IEEE Transactions on Automatic Control*, vol. 53, no. 4, pp. 1019-1025, 2008.

Chen, Z., and Tan, X. A control-oriented and physics-based model for ionic polymer-metal composite actuator. *IEEE Transactions on Mechatronics*, vol. 13, no. 5, pp. 519-529, 2008.

Chen, Z., and Tan, X. Monolithic fabrication of ionic polymer-metal composite actuators capable of complex deformation. *Sensors and Actuators A: Physical*, vol. 157, pp.246-257, 2010.

Croft, D., Shed, G. and Devasia, S. Creep, hysteresis, and vibration compensation for piezoactuators: atomic force microscopy application. *ASME Journal of Dynamic Systems, Measurement, and Control*, vol. 123, pp. 35-43, 2001.

Cross, R., Krasnosel'skii, M.A. and Pokrovskii, A.V. A time-dependent Preisach model. *Physica B*, vol. 306, pp. 206-210, 2001.

Gorbet, R.B., Morris, K., and Wang, D.W.L. Passivity-based stability and control of hysteresis in smart actuators. *IEEE Trans. on Control Systems Technology*, vol. 9, no. 1, pp. 5-16, 2001.

Guyer, R.A., McCall, K.R. and Boitnott, G.N. Hysteresis, discrete memory and nonlinear propagation in rock. *Phys. Rev. Lett.*, vol. 74, pp. 3491-3494, 1994.

Iyer R.V. and Shirley, M. Hysteresis parameter identification with limited experimental data. *IEEE Transactions on magnetics*, vol. 40, no. 5, pp. 3227-3239, 2004.

Krejci, P. and Kuhnen, K. Inverse control of systems with hysteresis and creep. *Proc. Inst. Elect. Eng. Control Theory Appl.*, vol. 148, pp. 185-192, 2001.

Kuhnen, K. and Janocha, H. Adaptive inverse control of piezoelectric actuators with hysteresis operators. *Proc. European Control Conference (ECC)*, Karlsruhe, Germany, 1999, paper F0291.

Moheimani, S.O.R. and Goodwin, G.C. Guest editorial introduction to the special issue on dynamics and control of smart structures. *IEEE Trans. on Control Systems Technology*, vol. 9, pp. 3-4, 2001.

Nemat-Nasser, S. and Li, J. Electromechanical response of ionic poly-metal composites. *Journal of Applied Physica*, vol. 87, pp. 3321-3331, 2000.

Natale, C., Velardi, F., and Visone, C. Identification and compensation of preisach hysteresis models for magnetostrictive actuators. *Physica B*, vol. 306, pp. 161-165, 2001.

Mayergoyz, I.D. *Mathematical Models of Hysteresis*. New York: Springer-Verlag, 1991.

Shahinpoor, M. and Kim, K. Ionic polymer-metal composite. Part I. Fundamentals. *Smart Materials and Structures*, vol. 10, pp. 819-833, 1991.

Su, C.-Y., Wang, Q., Chen, X. and Rakheja, S. Adaptive variable structure control of a class of nonlinear systems with unknown Prandtl-Ishlinskii hysteresis. *IEEE Transactions on Automatic Control*, vol. 50, no. 12, pp. 2069-2074, 2005.

Tao, G. and Kokotovic, P.V. Adaptive control of plants with unknown hysteresis. *IEEE Trans. on Automatic Control*, vol. 40, pp. 200-212, 1995.

Tan, X. and Baras, J.S. Modeling and control of hysteresis in magnetostrictive actuators. *Automatica*, vol. 40, no. 9, pp. 1469-1480, 2004.

Visintin, A. *Differential Models of Hysteresis*. New York: Springer-Verlag, 1994.

Webb, G.V., Lagoudas, D.C. and Kurdila, A.J. Hysteresis modeling of SMA actuators for control applications. *J. Intell. Mater. Syst. Struct.*, vol. 9, no. 6, pp. 432-448, 1998.